Electrical resistivity and oxidation behavior of Cu and Ti doped laser deposited high entropy alloys

Modupeola Dada and Patricia Popoola
Chemical, Metallurgical and Materials Engineering, Tshwane University of Technology, Pretoria, South Africa
Ntombi Mathe
Department of the National Laser Centre, Council for Scientific and Industrial Research, Pretoria, South Africa
Sisa Pityana
Chemical, Metallurgical and Materials Engineering, Tshwane University of Technology, Pretoria, South Africa and
Council for Scientific and Industrial Research, Pretoria, South Africa, and
Samson Adeosun
Metallurgical and Materials Engineering, University of Lagos, Lagos, Nigeria and
Department of Industrial Engineering, Durban University of Technology, Durban, South Africa

Abstract

Purpose – In this study, AlCoCrFeNi–Cu (Cu-based) and AlCoCrFeNi–Ti (Ti-based) high entropy alloys (HEAs) were fabricated using a direct blown powder technique via laser additive manufacturing on an A301 steel baseplate for aerospace applications. The purpose of this research is to investigate the electrical resistivity and oxidation behavior of the as-built copper (Cu)- and titanium (Ti)-based alloys and to understand the alloying effect, the HEAs core effects and the influence of laser parameters on the physical properties of the alloys.

Design/methodology/approach – The as-received AlCoCrFeNiCu and AlCoCrFeNiTi powders were used to fabricate HEA clads on an A301 steel baseplate preheated at 400°C using a 3 kW Rofin Sinar dY044 continuous-wave laser-deposition system fitted with a KUKA robotic arm. The deposits were sectioned using an electric cutting machine and prepared by standard metallographic methods to investigate the electrical and oxidation properties of the alloys.

Findings – The results showed that the laser power had the most influence on the physical properties of the alloys. The Ti-based alloy had better resistivity than the Cu-based alloy, whereas the Cu-based alloy had better oxidation residence than the Ti-based alloy which attributed to the compositional alloying effect (Cu, aluminum and nickel) and the orderliness of the lattice, which is significantly associated with the electron transportation; consequently, the more distorted the lattice, the easier the transportation of electrons and the better the properties of the HEAs.

Originality/value – It is evident from the studies that the composition of HEAs and the laser processing parameters are two significant factors that influence the physical properties of laser deposited HEAs for aerospace applications.

Keywords Laser deposition, Electrical resistivity, Oxidation, High entropy alloys

Paper type Research paper

Introduction

For over a decade, high entropy alloys (HEAs) have been extensively studied for aerospace applications attributed to their distinct design concept and properties. Conventional alloy designs were based on only one principal element called the base metal, with the addition of several alloying elements to improve the properties of the base metal, thus forming binary, tertiary and quaternary alloys. However, the innovative HEAs concept is based on at least five principal elements, with each element having a concentration between 35 and 5 at.%

The current issue and full text archive of this journal is available on Emerald Insight at: **https://www.emerald.com/insight/1708-5284.htm**

World Journal of Engineering
20/5 (2023) 868–876
Emerald Publishing Limited [ISSN 1708-5284]
[DOI 10.1108/WJE-09-2021-0523]

The authors would like to appreciate Mr Samuel Skhosane at the Council for Scientific and Research, the National Laser Center (Laser Enabled Manufacturing Resource Group), and Mr Juwon Ojo Fayomi and Uyor Uwa Orji at the Surface Engineering Research Laboratory, Tshwane University of Technology, Pretoria, South Africa, for their technical support during this research.

Received 7 September 2021
Revised 13 March 2022
Accepted 20 March 2022

(Yeh, 2004; He *et al.*, 2017). The HEA concept is very different from the traditional principal elemental approach of alloy development. HEAs can be made from minor elements with <5 at.% attributed to their solid solution phases and their higher mixing entropies (Tsai and Yeh, 2014). These characteristic solid solution phases give HEAs attractive properties such as excellent elevated temperature strength (Hsu *et al.*, 2011), hardness (Zhou *et al.*, 2007; Xin *et al.*, 2021), wear resistance (Chuang *et al.*, 2011; Jin *et al.*, 2018), corrosion resistance (Kao *et al.*, 2010), thermal stability (Tsai *et al.*, 2011; Chen *et al.*, 2019) and electrical and magnetic properties (Kao *et al.*, 2011). According to Arif *et al.* (2021), HEAs are potential materials for several applications and industries such as petrochemical, canning and bottling industries, nuclear fusion and fission reactors, energy storage, automobile, biomedical, marine equipment and aerospace turbine blades application (Arif *et al.*, 2022; Maulik *et al.*, 2018). AlCoCrFeNi HEA is one of the most studied compositions, which acts as an excellent binder owing to its high entropy mixing effect (Zhu *et al.*, 2013). Properties of this alloying system can be improved with the inclusion of other alloying elements. The influence of adding Nb to the AlCoCrFeNi HEA composition was investigated (Ma and Zhang, 2012). The authors mentioned that the alloy's microhardness and yield strength increased linearly with an increase in Nb content. In another study, the effect of vanadium on the properties of AlCoCrFeNi HEA composition was examined; the authors recorded an increase in the plastic strain, microhardness and compressive strength of the alloy with an increase in the vanadium content (Dong *et al.*, 2014). The minor addition of Zr to the AlCoCrFeNi HEA composition was reported to have significantly increased the mechanical properties of the alloy (Chen *et al.*, 2016). The influence of copper (Cu) on the mechanical and microstructural properties of the AlCoCrFeNi HEA composition was examined. The results showed that Cu influenced the face centred cubic (FCC) phase formation, with an increase in the yield strength and reduction in the plastic strain as the Cu content increased (Zhu *et al.*, 2016). The effect of titanium (Ti) on the mechanical properties of the AlCoCrFeNi HEA was tested. The results showed that the alloy had a dendritic phase with a body centred cubic (BCC) structure. The hardness and yield strength increased as the Ti content increased and the authors attributed the increment to the solid solution strengthening mechanism of the Ti addition to the HEA (Wang *et al.*, 2013).

Nonetheless, most studies in the literature on the AlCoCrFeNi HEAs compositional system with Cu and Ti additions are focused on the mechanical properties with limited reports on the electrical and thermal properties (Qiao *et al.*, 2021; Kang *et al.*, 2018). The physical properties of HEAs are still in their preliminary stages, with the mechanism of the composition and properties of the alloys being unclear, thus causing difficulties in controlling these properties which makes the reports on the phonon and electronic band structure of HEAs limited in the literature and should be explored (Tsai, 2013). Few studies investigated the relative contribution of the phonon and electron to the thermal conductivity and electrical resistivity of arc melted Al_xCoCrFeNi (Chou *et al.*, 2009). The authors argued that the phonon and electron components in the HEA are comparable with some conventional metals but need further studies. Furthermore, the authors reported a new class of soft magnetic material using HEAs (Zhang *et al.*, 2013). The electrical properties of $FeCoNi(AlSi)_x$ with the molar ratio of x from 0 to 0.8 via arc melting was investigated. The results showed that the HEAs had an optimum balance of properties at $x = 0.2$ with electrical resistivity of 69.5 $\mu\Omega \cdot$ cm. The electrical properties of as-cast Al_xCoCrFeNi were also analyzed and the results showed that the residual electrical resistivity of the HEAs varied between 100 and 200 $\mu\Omega \cdot$ cm (Kao *et al.*, 2011).

The improvement of the thermal properties of HEAs is essential for nuclear power plants vehicle and aero engines. These improvements can be attributed to the addition of alloying elements (Waseem and Ryu, 2020). Alloying elements such as Si, aluminum (Al) and chromium (Cr) form protective oxides like Cr_2O_3, SiO_2 and Al_2O_3 which improve the oxidation properties of HEA compositions (Zelenitsas and Tsakiropoulos, 2006; Cai *et al.*, 2019). Hence, the influence of Al on the oxidation behavior of $FeCoCrNiMnAl_x$ ($0 \leq x \leq 0.75$) HEA via laser-deposition method, was examined in air at 600°C. It was observed that the weight gain decreased with an increase in the volume fraction of Al attributed to the α-Al_2O_3 oxide formed at $FeCoCrNiMnAl_{0.5}$ and $FeCoCrNiMnAl_{0.75}$, respectively (Cui *et al.*, 2020a). However, the α-Al_2O_3 oxide scale formed had poor adhesion to the surface of the alloy. Furthermore, the oxidation properties of Al–Co–Cr–Ni–(Fe, Si) HEAs at elevated temperatures were studied. At low Al content, Cr_2O_3 oxide scale was observed on the outside surface of the HEA, whereas AlN and Al_2O_3 precipitates were observed internally (Butler *et al.*, 2015). At higher Al content, small mass grains with Al_2O_3 scales were observed externally.

In another study, the effect of iron on the oxidation performance of Fe_xCoCrNi HEA coating was investigated at 950°C. After 5 and 100 h, the results showed that the high temperature oxidation resistance of the alloy was decreased with an increase in volume fraction of iron (Fe) attributed to the formation of Fe_2O_3 oxide on the outer side of the coating (Cai *et al.*, 2018). Another study probed the effect of Cu on the oxidation behavior of arc-melted $AlCoCrCu_xFe$ HEAs (Dąbrowa *et al.*, 2017). The results showed that the oxidation resistance reduced with an increase in Cu content with drastic changes noticed in the microstructure between 100 and 500 h attributed to the tendency of Cu to segregate, which severely influenced the oxidation behavior of the alloy (Singh *et al.*, 2011; Tung *et al.*, 2007; Wen *et al.*, 2009).

The $Al_{0.5}$CrCoFeNi HEA was fabricated via arc melting and the oxidation resistance of the alloy at several temperatures and compositions for 100 h was investigated (Lihua *et al.*, 2015). The results showed excellent oxidation resistance at 800°C and 900°C; however, a decline in oxidation resistance was observed as the temperature increased from 1,000°C to 1,100°C. The oxidation behavior of the alloy followed the parabolic law at 800°C and 900°C. Nonetheless, at 1,000°C, the alloy showed both a linear oxidation rate and a parabolic rate law at $x = 0.97$ and 0.56, respectively (Abbaszadeh *et al.*, 2020). The oxidation rate of CrMnFeCoNi HEA was noticed to be both linear and parabolic at 500°C–900°C. The oxides formed at 700°C and 800°C were Cr enriched Mn_2O_3 and a Cr_2O_3 thin layer, whereas Mn_3O_4 oxides were formed at 900°C (Laplanche *et al.*, 2016). Chang *et al.* (2019) also studied the influence of Cr on the laser-deposited $FeCr_xCoNiB$ HEA where $0.5 \leq x \leq 3.0$ and the authors stated that the oxidation characteristics of the coating was

improved, attributed to the Cr_2O_3, $CoFe_2O_4$ and Fe_2O_3 oxides formed on the surface of the coating. Consequently, the addition of alloying element and fabrication technique will significantly alter the physical properties of HEAs (Amendola *et al.*, 2015; Alaneme *et al.*, 2016; Farina *et al.*, 2016).

Cui *et al.* (2020b) and Xu *et al.* (2020a) studied the oxidation behavior and the influence of Ti in $AlCoCrFeNiTi_{0.5}$ laser-deposited HEAs and the influence of Cu in CuAlNiCrFe laser-deposited HEAs, respectively; however, there are limited literature reports on the electrical resistivity and oxidation behavior of AlCoCrFeNi HEAs with regard to the comparative influence of Cu and Ti alloying elements on the physical properties of AlCoCrFeNi–Cu and AlCoCrFeNi–Ti laser deposited HEAs. Therefore, this study comparatively investigates the physical properties of AlCoCrFeNi–Cu (Cu-based) and AlCoCrFeNi–Ti (Ti-based) HEAs fabricated via laser additive manufacturing to understand the influence of alloying elements on the physical properties of the HEAs and investigates the potential application of these as-built alloys in the aerospace industry.

Materials and methods

Sample preparation

Baseplates with dimension 50 × 50 × 5 mm were sandblasted with silica grit using SBC 350 vertical sandblasting machine and wiped clean with acetone to increase the laser absorption and reduce laser reflection during deposition. There were no infringements of human or animal rights during fabrication. Table 1 shows the chemical composition of the HEA powder with an average particle size of 45–106 μm comprising Al, cobalt (Co), Cr, Fe, nickel (Ni), Cu and Ti having (99.9%) purity which were mixed together to form AlCoCrFeNiCu (Cu-based) and AlCoCrFeNiTi (Ti-based) HEAs via gas atomization and supplied by F.J. Brodmann & Co., L.L.C., USA. The powder particle size resulted in good flowability during deposition. The as-received powders shown in Figure 1(a) and (b) having flake irregular and spherical shapes were used to fabricate HEA on an A301 steel baseplate preheated at 400°C using a 3 kW Rofin Sinar dY044 continuous-wave laser-deposition system fitted with a KUKA robotic arm. The optimized laser processing parameters shown in Table 2 were extracted from previous studies at 1,400–1,600 W, a beam spot size at 2 mm, argon gas flow rate at 1.2 L/min and scan speed at 10–12 mm/s (Dada *et al.*, 2020). Multiple tracks were produced at 50% overlap and 45° to the base plate.

Microstructural analysis

The microstructural characterization of the as-built HEAs samples was achieved using a Jeol-JSM-7600F Field Emission Scanning Electron Microscope fitted with an energy dispersive spectroscopy after etching with aqua regia.

Thermal oxidation analysis

The oxidation behavior of the as-built HEAs was investigated using a thermal gravimetric analyzer. The alloys were studied at an initial temperature of 400°C and final temperature at 900°C with heating rate of 10°C/min in 20 mL/min air.

Electrical resistivity and conductivity analysis

The electrical resistivity and conductivity of the as-built HEAs were determined using a four-point probe meter (HP2662, China) at different laser parameters. The current was set at 100 mA and the speed was set at 7 times/min. The electrical resistivity of each samples were extracted and the inverse of each resistivity value resulted in the electrical conductivities of the as-built samples.

Results and discussion

Thermal oxidation properties

The as-built HEAs samples were produced via laser-metal deposition on a steel baseplate using familiar laser processing parameters. The cross-sectional structures of the deposits showed the HEAs had uniformity in each elemental

Table 1 Chemical composition of the Cu- and Ti-based HEA

Element	Al (at.%)	Co (at.%)	Cr (at.%)	Fe (at.%)	Ni (at.%)	Cu (at.%)	Ti (at.%)
Nominal	16.6	16.6	16.6	16.6	16.6	16.6	16.6
Cu-based HEA	42.95	11.09	10.24	13.52	10.36	11.84	–
Ti-based HEA	44.12	10.23	10.96	12.55	10.96		11.18

Figure 1 SEM micrograph of the powder morphology

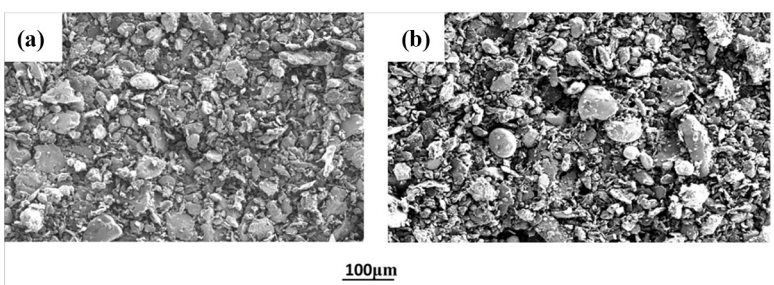

Notes: (a) Ti-based HEA; (b) Cu-based HEA

Table 2 Optimized laser processing parameters

High entropy alloys	Sample	Laser power (W) (J/s)	Scan speed (V) (mm/s)	Beam diameter (mm)	Energy density $E = (P/V^*d)$ (J/mm^2)
Cu based	A	1,400	12	2	58.3
	B	1,600	10	2	80
Ti based	C	1,400	12	2	58.3
	D	1,600	10	2	80

Figure 2 Representative SEM micrograph of laser deposited HEA clad

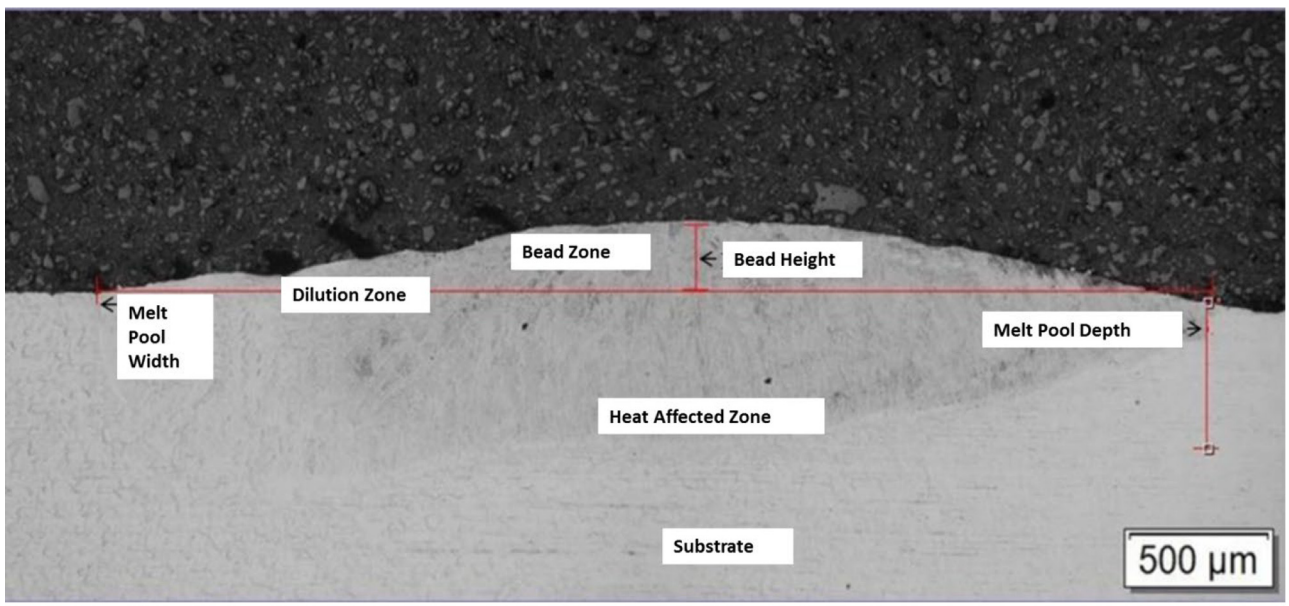

Note: Dada *et al.*, 2020

composition and that the thickness of the clad was between 500 and 1,000mm for all alloys, comprising clad-zone, bond-zone and heat-affected zone with no obvious microstructural defects as shown in Figure 2.

The bonding line at the interface of the coating was clear and smooth, showing good metallurgical bonding between the baseplate and the HEAs (Liu *et al.*, 2014). The XRD patterns shown in Figure 3 of the laser-deposited HEAs AlCoCrFeNiCu and AlCoCrFeNiTi reveal the alloys were composed of FCC and BCC phases with the AlCoCrFeNiTi having more predominant peaks with BCC structures than the AlCoCrFeNiCu HEA attributed to the alloying compositional effect.

According to these observations, the volume fraction of the BCC phase in both alloys more than the FCC phase attributed to the rapid solidification feature of the laser-deposition process (Ocelík *et al.*, 2016). The alloys had excellent metallurgical bond without defects. The two samples of the Cu-based and the Ti-based HEAs each showed columnar and equiaxed dendritic microstructures, respectively, attributed to the heat flux direction and rapid solidification process of manufacturing route shown in Figure 4 (Xu *et al.*, 2020b). Similar grain morphologies were observed in other laser-deposited HEAs (Xiang *et al.*, 2019a, 2019b).

The oxidation behavior of the HEAs was investigated in air using PerkinElmer Thermogravimetric Analyzer (TGA 4000). Thermal gravimetric analyzer can be used to determine the thermal stability of the HEAs under a constant heating rate in an inert environment. The variations in weight as a function of temperatures between 37°C and 1,000°C and constant heat rate of 20 C · min^{-1} are shown in Figure 5.

The results show that the resistance to oxidation can be ranked as sample A > D>C > B in order of the smallest to the largest mass. The Cu-based HEA at 1,400 W and 12 mm/s had the smallest mass suggesting the alloy had the best oxidation resistance. The percentage weight change for each composition is displayed in Figure 6.

Samples C and D exhibited the highest weight change at 0.3% and 0.27%, respectively, attributed to the compositional effect. The Ti-based HEA experienced selective oxidation because of the high affinity Ti has for oxygen at high temperatures, making the alloying composition oxidize more rapidly than the Cu-based HEA (Guleryuz and Cimenoglu, 2009). The laser parameters also influenced the weight difference of the alloys, increasing with an increase in laser power from 1,400 to 1,600 W. The energy density, which increased from 58.3 J/mm2 to 80 J/mm^2 at 1,400 W to 1,600 W, was adequate to support the thermodynamic formation of solid solution phases that are resistant to thermal decomposition (Fargas *et al.*, 2017). The high amount of Al in both alloys promotes the formation of Al_20_3 protective scales showing

Figure 3 XRD graph of laser deposited

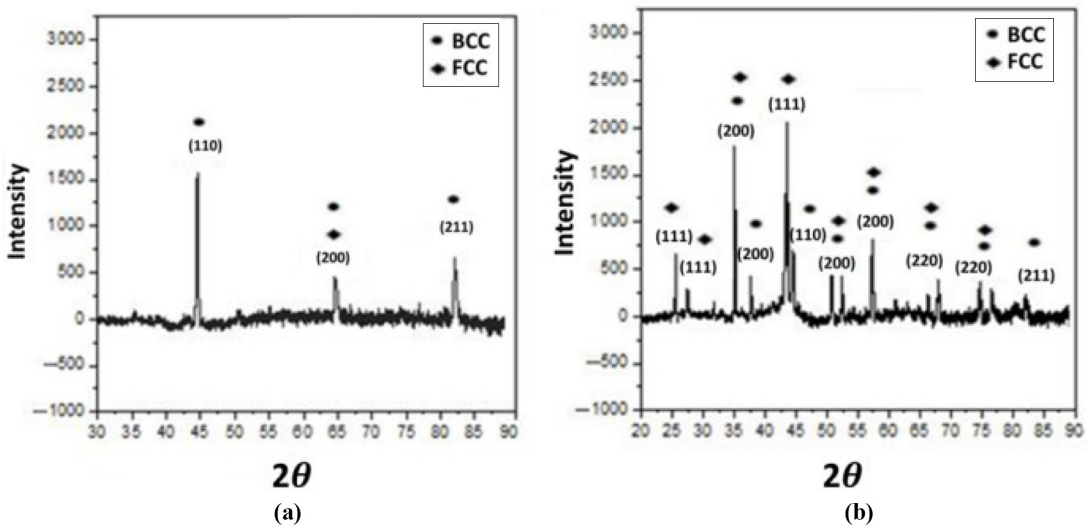

Notes: (a) Cu-based; (b) Ti-based HEA at 1,600 W and 10 mm/s

Figure 4 Microstructure of as-built HEAs

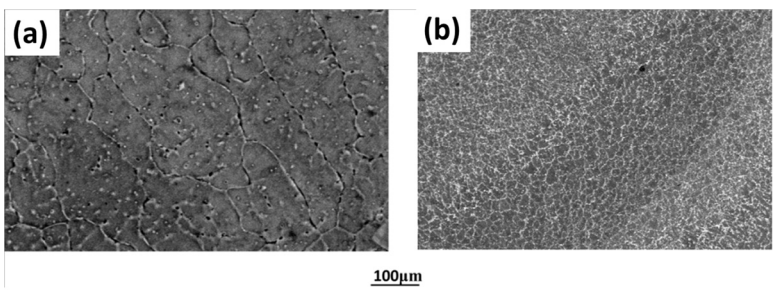

Notes: (a) Cu-based columnar dendrite structure; (b) Ti-based equiaxed dendrite structure

Figure 5 Oxidation behavior of the Cu- and Ti-based high entropy alloys

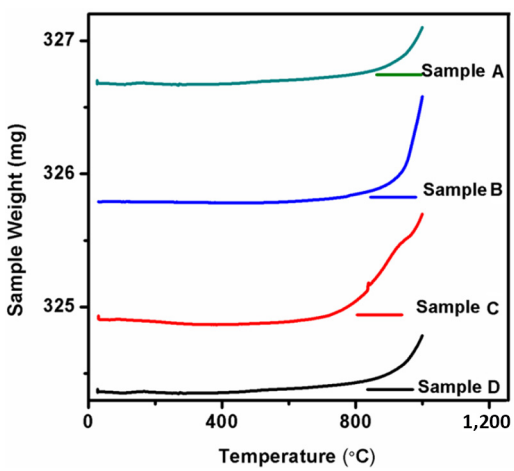

Figure 6 Comparative weight change of the Cu- and Ti-based high entropy alloys

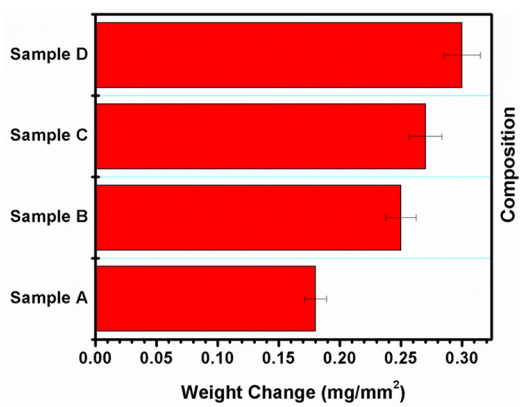

similarities with stainless steels (Xu *et al.*, 2011; Pint *et al.*, 2007; Brady *et al.*, 2008). In general, both HEAs had good oxidation resistance with a parabolic growth rate attributed to the lattice distortion effect from the high concentration of alloying elements

Table 3 Summary of the compositional effect on the oxidation behavior of high entropy alloys and their fabrication techniques

High entropy alloy	Condition of exposure	Fabrication technique	Results	Ref.
AlCoCrFeNiCu and AlCoCrFeNiTi Studying the effect of Cu and Ti	1,000°C Thermal gravimetric analyzer	Laser deposition	High Al content, with continuous and protective Al_2O_3 scale observed obeying parabolic growth law. Cu-based had better oxidation than the Ti-based alloy	This study
$Al_{0.6}$CoCrCuFeNi and $Al_{0.6}$CoCrCuFeNi$Si_{0.3}$ Studying the effect of Si	800°C–1,000°C Furnace exposure	Arc melting	Cr_2O_3/spinel and Al_2O_3 oxide observed. The effect of Si positively influenced the oxidation behavior only at 800°C	Chen *et al.* (2018)
Al_xCoCrFeNiTi_y $Al_{0.5}$CoCrFeNi AlCoCrFeNi$Ti_{0.5}$ Studying the effect of Al and Ti	1,000°C Furnace exposure	Induction melting	Al and Ti oxides. Al improves oxidation, whereas Ti deteriorates oxidation	Erdogan *et al.* (2019)
AlCoCrFeNiCu_x Studying the effect of Cu	1,000°C Thermal gravimetric analyzer	Arc melting	α-Al_2O_3 oxide formed, spallation with increase in Cu content and phase changes observed	Dąbrowa *et al.* (2017)
$Al_{0.8}$CoCrSiNi and $Al_{0.44}$CoCrFeNi Studying the effect of Al	Furnace exposure at 1,050°C	Casting	With low Al content Cr_2O_3, high Al content Al_2O_3 scale obeying parabolic growth law	Butler *et al.* (2015)
AlCoCrFeNi$Ti_{0.5}$	Electric furnace at 700°C and 800°C	Laser metal deposition	Cr_2O_3 and Al_2O_3 oxides were formed attributed to the improvement of the oxidation resistance	Cui *et al.* (2020)
AlCrCuFeNi	Industrial tube furnace at 1,050°C	Laser cladding	α-Al_2O_3 oxide was formed which prevented the formation of spinel structures and other oxides	Xu *et al.* (2020)

such as Al, which significantly reduces the diffusivity, thus, prolonging the growth of oxide layers and improving the oxidation resistance (Butler and Weaver, 2016). Some studies in the literature and their results are summarized in Table 3. It was observed that the studies on the oxidation behavior of laser-deposited HEAs were focused on the influence of alloying elements on the thermal properties of the HEAs, hence, showing that alloying elements play a significant role in improving the properties of HEAs and provides proper guidance to future design and development of HEAs (Tong *et al.*, 2020).

Electrical resistivity and conductivity properties

The electrical resistivity of the HEAs was measured at room temperature. The values of resistivity were inversed to derive the electrical conductivity, σ of the alloys (Amendola *et al.*, 2015). The resistivity of the laser-deposited HEAs in this study is relatively higher than those in the literature fabricated by casting technique attributed to the rapid solidification of the additive manufacturing process, which causes a high distortion of the lattice promoting the scattering of electron waves in the as-built HEA system (Zhu *et al.*, 2013). Generally, the electrical resistivity of most materials is controlled by the composition and temperature. However, the resistivity of the HEAs is influenced by the phonon (T^3), electron–electron interaction ($T^{1/2}$), temperature (T) and the magnetic effect (T^2), but at intermediate temperatures of about 200 k, the electrical resistivity is mostly influenced by the temperature and magnetic effect, whereas at temperatures between 300 and 400 k, the resistivity is influenced only by the phonon (Alaneme *et al.*, 2016). The graph of electrical resistivity, electrical conductivity and International Annealed Copper Standard (IACS) as a function of the composition and laser parameter is shown in Figure 7. Electrical resistivity is influenced by the composition and temperature (Zhu *et al.*, 2013). The results showed that resistivity increases with an increase in laser power in both alloys. The resistivity of the Ti-based HEA at 3.6×10^{-6} Ωm was higher than that of the Cu-based HEA at 2.9×10^{-6} Ωm attributed to the compositional effect. Ti has about 3% conductivity as Cu with much higher resistivity. The atomic bonding of the Ti-based HEA is improved attributed to the predominant BCC solid solution phase which was more observed in the Ti-based HEA, thus improving the electrical resistivity of the alloy (Jin *et al.*, 2018).

Figure 7 Electrical resistivity, conductivity and IACS plots for the Cu- and Ti-based high entropy alloys

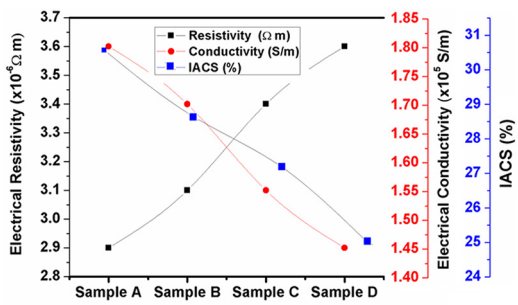

On the other hand, Cu in the Cu-based HEA had the highest electrical conductivity at $1.8 \times \times 10^5$ (31% IACS) attributed to the compositional effect of Cu, Al and Ni alongside the orderliness of the lattice, which is significantly associated with the electron transportation. Therefore, the more distorted the lattice, the easier the transportation of electrons. Free electron movement in the lattice influences the increment of the electrical conductivity (Farina *et al.*, 2016). Therefore, energy is transmitted better in the Cu-based HEA than the Ti-based HEA. Comparatively, the chart in Figure 8 shows that the Ti-based HEA generally had the better physical properties compared with the Cu-based HEA, whereas the comparative electrical resistivity values of HEAs and their various fabrication techniques are shown in Table 4.

Conclusion

In this study AlCoCrFeNi–Cu (Cu-based) and AlCoCrFeNi–Ti (Ti-based) HEAs were fabricated using a direct blown powder technique via laser additive manufacturing on an A301 steel baseplate. The thermal properties, the electrical resistivity and thermal conductivity of the as-built Cu- and Ti-based alloys were investigated to understand the compositional effect, the high entropy core effect and the effect of the laser processing parameters on the physical properties of the alloys.

Figure 8 Chart showing the physical properties of the Cu-based HEAs (samples A and B) and Ti-based HEAs (samples C and D)

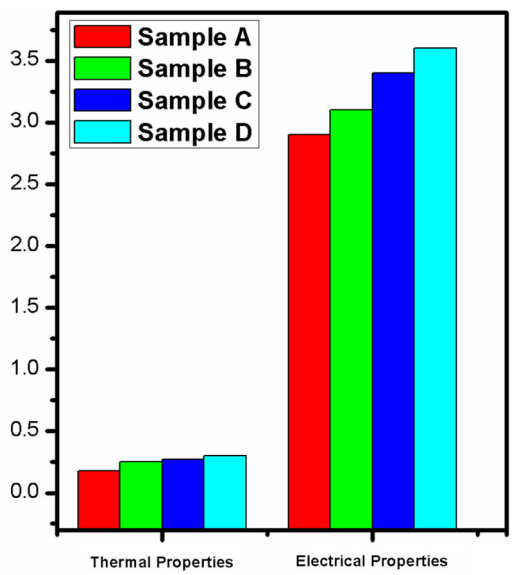

Table 4 Electrical resistivity of high entropy alloys and their fabrication techniques

High entropy alloy	Resistivity	Fabrication technique	Ref.
AlCoCrFeNi	1.42 Ωm	Casting	Kao *et al.* (2011)
AlCoCrFeNiCu	2.9 Ωm	Laser deposition	This study
CoCrFeNi	2.21 Ωm	Casting	Kao *et al.* (2011)
AlCoCrFeNiTi	3.6 Ωm	Laser deposition	This study
Al_2CoCrFeNi	2.11 Ωm	Casting	Kao *et al.* (2011)

The Cu-based HEA had slightly better oxidation properties, whereas the Ti-based HEA had better resistivity attributed to the compositional effect. The Ti-based HEA experienced selective oxidation because of the high affinity Ti has for oxygen at high temperatures, making the alloying composition oxidize more rapidly than the Cu-based HEA. The lattice distortion effect had the most influence on the physical properties of the laser-deposited HEAs, which invariably promotes the scattering of electron and phonons waves that increase the resistivity and reduce the thermal conductivity. Also, the laser power had the most effect on the resistivity of both alloys, increases with an increase in laser power. Generally, the physical properties of as-built HEAs were significantly influenced by the variation of alloying elements. Nonetheless, more studies need to be done on the cost implication of the compositional combination of both alloys and the influence of heat treatment on the physical properties of the as-built HEAs.

References

Abbaszadeh, S., *et al.* (2020), "Investigation of the high-temperature oxidation behavior of the Al0. 5CoCrFeNi high entropy alloy", *Surfaces and Interfaces*, Vol. 21, p. 100724.

Alaneme, K.K., Bodunrin, M.O. and Oke, S.R. (2016), "Processing, alloy composition and phase transition effect on the mechanical and corrosion properties of high entropy alloys: a review", *Journal of Materials Research and Technology*, Vol. 5 No. 4, pp. 384-393.

Amendola, A., Hernández-Nava, E., Goodall, R., Todd, I., Skelton, R.E. and Fraternali, F. (2015), "On the additive manufacturing, post-tensioning and testing of bi-material tensegrity structures", *Composite Structures*, Vol. 131, pp. 66-71.

Arif, Z.U., Khalid, M.Y., ur Rehman, E., Ullah, S., Atif, M. and Tariq, A. (2021), "A review on laser cladding of high-entropy alloys, their recent trends and potential applications", *Journal of Manufacturing Processes*, Vol. 68, pp. 225-273.

Arif, Z.U., Khalid, M.Y., Al Rashid, A., ur Rehman, E. and Atif, M. (2022), *Laser Deposition of High-Entropy Alloys: A Comprehensive Review. Optics & Laser Technology*, Vol. 145, p. 107447.

Brady, M.P., Yamamoto, Y., Santella, M.L., Maziasz, P.J., Pint, B. A., Liu, C.T., Lu, Z.P. and Bei, H. (2008), "The development of alumina-forming austenitic stainless steels for high-temperature structural use", *JOM*, Vol. 60 No. 7, pp. 12-18.

Butler, T.M. and Weaver, M.L. (2016), "Oxidation behavior of arc melted AlCoCrFeNi multi-component high-entropy alloys", *Journal of Alloys and Compounds*, Vol. 674, pp. 229-244.

Butler, T.M., Alfano, J.P., Martens, R.L. and Weaver, M.L. (2015), "High-temperature oxidation behavior of Al-Co-Cr-Ni-(Fe or Si) multicomponent high-entropy alloys", *JOM*, Vol. 67 No. 1, pp. 246-259.

Cai, Y., Chen, Y., Manladan, S.M., Luo, Z., Gao, F. and Li, L. (2018), "Influence of dilution rate on the microstructure and properties of FeCrCoNi high-entropy alloy coating", *Materials & Design*, Vol. 142, pp. 124-137.

Cai, Y., Zhu, L., Cui, Y., Geng, K., Manladan, S.M. and Luo, Z. (2019), "High-temperature oxidation behavior of FeCoCrNiAlx high-entropy alloy coatings", *Materials Research Express*, Vol. 6 No. 12, p. 126552.

Chang, F., Cai, B., Zhang, C., Huang, B., Li, S. and Dai, P. (2019), "Thermal stability and oxidation resistance of

FeCrxCoNiB high-entropy alloys coatings by laser cladding", *Surface and Coatings Technology*, Vol. 359, pp. 132-140.

Chen, J., Niu, P., Liu, Y., Lu, Y., Wang, X., Peng, Y. and Liu, J. (2016), "Effect of Zr content on microstructure and mechanical properties of AlCoCrFeNi high entropy alloy", *Materials & Design*, Vol. 94, pp. 39-44.

Chen, C., Liu, N., Zhang, J., Cao, J., Wang, L.J. and Xiang, H.F. (2019), "Microstructure stability and oxidation behaviour of (FeCoNiMo) 90 (Al/Cr) 10 high-entropy alloys", *Materials Science and Technology*, Vol. 35 No. 15, pp. 1883-1890.

Chen, L., Zhou, Z., Tan, Z., He, D., Bobzin, K., Zhao, L., Oete, M. and Königstein, T. (2018), "High temperature oxidation behavior of Al0. 6CrFeCoNi and Al0. 6CrFeCoNiSi0.3 high entropy alloys", *Journal of Alloys and Compounds*, Vol. 764, pp. 845-852.

Chou, H.-P., Chang, Y.S., Chen, S.K. and Yeh, J.W. (2009), "Microstructure, thermophysical and electrical properties in AlxCoCrFeNi (0≤ x≤ 2) high-entropy alloys", *Materials Science and Engineering: B*, Vol. 163 No. 3, pp. 184-189.

Chuang, M.H., Tsai, M.H., Wang, W.R., Lin, S.J. and Yeh, J.W. (2011), "Microstructure and wear behavior of AlxCo1. 5CrFeNi1. 5Tiy high-entropy alloys", *Acta Materialia*, Vol. 59 No. 16, pp. 6308-6317.

Cui, W., Li, W., Chen, W.T. and Liou, F. (2020a), "Laser metal deposition of an AlCoCrFeNiTi0. 5 high-entropy alloy coating on a Ti6Al4V substrate: microstructure and oxidation behavior", *Crystals*, Vol. 10 No. 8, pp. 638.

Cui, Y., Shen, J., Manladan, S.M., Geng, K. and Hu, S. (2020b), "Wear resistance of FeCoCrNiMnAlx high-entropy alloy coatings at high temperature", *Applied Surface Science*, Vol. 512, p. 145736.

Dąbrowa, J., Cieślak, G., Stygar, M., Mroczka, K., Berent, K., Kulik, T. and Danielewski, M. (2017), "Influence of Cu content on high temperature oxidation behavior of AlCoCrCuxFeNi high entropy alloys (x= 0; 0.5; 1)", *Intermetallics*, Vol. 84, pp. 52-61.

Dada, M., Popoola, P., Mathe, N., Pityana, S., Adeosun, S., Aramide, O. and Lengopeng, T. (2020), "Process optimization of high entropy alloys by laser additive manufacturing", *Engineering Reports*, Vol. 2 No. 10, p. e12252.

Dong, Y., Zhou, K., Lu, Y., Gao, X., Wang, T. and Li, T. (2014), "Effect of vanadium addition on the microstructure and properties of AlCoCrFeNi high entropy alloy", *Materials & Design*, Vol. 57, pp. 67-72.

Erdogan, A., Doleker, K.M. and Zeytin, S. (2019), "Effect of Al and Ti on high-temperature oxidation behavior of CoCrFeNi-based high-entropy alloys", *JOM*, Vol. 71 No. 10, pp. 3499-3510.

Fargas, G., Roa, J.J., Sefer, B., Pederson, R., Antti, M.L. and Mateo, A. (2017), "Oxidation behavior of TI-6Al-4V alloy exposed to isothermal and cyclic thermal treatments", *26th International Conference on Metallurgy and Materials METAL 2017*, *Brno, Czech Republic*, May 24th-26th, 2017. TANGER Ltd.

Farina, I., Fabbrocino, F., Carpentieri, G., Modano, M., Amendola, A., Goodall, R., Feo, L. and Fraternali, F. (2016), "n the reinforcement of cement mortars through 3D printed polymeric and metallic fibers", *Composites Part B: Engineering*, Vol. 90, pp. 76-85.

Guleryuz, H. and Cimenoglu, H. (2009), "Oxidation of Ti–6Al–4V alloy", *Journal of Alloys and Compounds*, Vol. 472 Nos 1/2, pp. 241-246.

He, Q., Ding, Z.Y., Ye, Y.F. and Yang, Y. (2017), "Design of high-entropy alloy: a perspective from nonideal mixing", *JOM*, Vol. 69 No. 11, pp. 2092-2098.

Hsu, C.Y., Juan, C.C., Wang, W.R., Sheu, T.S., Yeh, J.W. and Chen, S.K. (2011), "On the superior hot hardness and softening resistance of AlCoCrxFeMo0. 5Ni high-entropy alloys", *Materials Science and Engineering: A*, Vol. 528 Nos 10/11, pp. 3581-3588.

Jin, G., Cai, Z., Guan, Y., Cui, X., Liu, Z., Li, Y. and Dong, M. (2018), "High temperature wear performance of laser-cladded FeNiCoAlCu high-entropy alloy coating", *Applied Surface Science*, Vol. 445, pp. 113-122.

Kang, M., Lim, K.R., Won, J.W. and Na, Y.S. (2018), "Effect of Co content on the mechanical properties of A2 and B2 phases in AlCoxCrFeNi high-entropy alloys", *Journal of Alloys and Compounds*, Vol. 769, pp. 808-812.

Kao, Y.F., Lee, T.D., Chen, S.K. and Chang, Y.S. (2010), "Electrochemical passive properties of AlxCoCrFeNi (x= 0, 0.25, 0.50, 1.00) alloys in sulfuric acids", *Corrosion Science*, Vol. 52 No. 3, pp. 1026-1034.

Kao, Y.F., Chen, S.K., Chen, T.J., Chu, P.C., Yeh, J.W. and Lin, S.J. (2011), "Electrical, magnetic, and hall properties of AlxCoCrFeNi high-entropy alloys", *Journal of Alloys and Compounds*, Vol. 509 No. 5, pp. 1607-1614.

Laplanche, G., Volkert, U.F., Eggeler, G. and George, E.P. (2016), "Oxidation behavior of the CrMnFeCoNi high-entropy alloy", *Oxidation of Metals*, Vol. 85 Nos 5/6, pp. 629-645.

Lihua, H., Hua, Z., Qunhua, T., Jiancheng, W. and Pinqiang, D. (2015), "High temperature oxidation behavior of Al0. 5CrCoFeNi high entropy alloy. ", *Rare Metal Materials and Engineering*, Vol. 44 No. 2, pp. 424-428.

Liu, C., Wang, H.M., Zhang, S.Q., Tang, H.B. and Zhang, A.L. (2014), "Microstructure and oxidation behavior of new refractory high entropy alloys", *Journal of Alloys and Compounds*, Vol. 583, pp. 162-169.

Ma, S. and Zhang, Y. (2012), "Effect of Nb addition on the microstructure and properties of AlCoCrFeNi high-entropy alloy", *Materials Science and Engineering: A*, Vol. 532, pp. 480-486.

Maulik, O., Kumar, D., Kumar, S., Dewangan, S.K. and Kumar, V. (2018), "Structure and properties of lightweight high entropy alloys: a brief review", *Materials Research Express*, Vol. 5 No. 5, p. 052001.

Ocelík, V., Janssen, N., Smith, S.N. and De Hosson, J.T.M. (2016), "Additive manufacturing of high-entropy alloys by laser processing", *JOM*, Vol. 68 No. 7, pp. 1810-1818.

Pint, B.A., Shingledecker, J.P., Brady, M.P. and Maziasz, P.J. (2007), "Alumina-forming austenitic alloys for advanced recuperators", *In Turbo Expo: Power for Land, Sea, and Air*, Vol. 47926, pp. 995-1002.

Qiao, L., Liu, Y. and Zhu, J. (2021), "A focused review on machine learning aided high-throughput methods in high entropy alloy", *Journal of Alloys and Compounds*, Vol. 877, p. 160295.

Singh, S., Wanderka, N., Murty, B.S., Glatzel, U. and Banhart, J. (2011), "Decomposition in multi-component

AlCoCrCuFeNi high-entropy alloy", *Acta Materialia*, Vol. 59 No. 1, pp. 182-190.

Tong, Y., Bai, L., Liang, X., Chen, Y., Zhang, Z., Liu, J., Li, Y. and Hu, Y. (2020), "Influence of alloying elements on mechanical and electronic properties of NbMoTaWX (X= Cr, Zr, V, Hf and Re) refractory high entropy alloys", *Intermetallics*, Vol. 126, p. 106928.

Tsai, M.H. (2013), "Physical properties of high entropy alloys", *Entropy*, Vol. 15 No. 12, pp. 5338-5345.

Tsai, M.H. and Yeh, J.W. (2014), "High-entropy alloys: a critical review", *Materials Research Letters*, Vol. 2 No. 3, pp. 107-123.

Tsai, M.H., Wang, C.W., Tsai, C.W., Shen, W.J., Yeh, J.W., Gan, J.Y. and Wu, W.W. (2011), "Thermal stability and performance of NbSiTaTiZr high-entropy alloy barrier for copper metallization", *Journal of the Electrochemical Society*, Vol. 158 No. 11, p. H1161.

Tung, C.C., Yeh, J.W., Shun, T.T., Chen, S.K., Huang, Y.S. and Chen, H.C. (2007), "On the elemental effect of AlCoCrCuFeNi high-entropy alloy system", *Materials Letters*, Vol. 61 No. 1, pp. 1-5.

Wang, Y., Ma, S., Chen, X., Shi, J., Zhang, Y. and Qiao, J. (2013), "Optimizing mechanical properties of AlCoCrFeNiTi x high-entropy alloys by tailoring microstructures", *Acta Metallurgica Sinica (English Letters)*, Vol. 26 No. 3, pp. 277-284.

Waseem, O.A. and Ryu, H.J. (2020), "Combinatorial synthesis and analysis of AlxTayVz-Cr20Mo20Nb20Ti20Zr10 and Al10CrMoxNbTiZr10 refractory high-entropy alloys: oxidation behavior", *Journal of Alloys and Compounds*, Vol. 828, p. 154427.

Wen, L., Kou, H.C., Li, J.S., Chang, H., Xue, X.Y. and Zhou, L. (2009), "Effect of aging temperature on microstructure and properties of AlCoCrCuFeNi high-entropy alloy", *Intermetallics*, Vol. 17 No. 4, pp. 266-269.

Xiang, S., Li, J., Luan, H., Amar, A., Lu, S., Li, K., Zhang, L., Liu, X., Le, G., Wang, X. and Qu, F. (2019a), "Effects of process parameters on microstructures and tensile properties of laser melting deposited CrMnFeCoNi high entropy alloys", *Materials Science and Engineering: A*, Vol. 743, pp. 412-417.

Xiang, S., Luan, H., Wu, J., Yao, K.F., Li, J., Liu, X., Tian, Y., Mao, W., Bai, H., Le, G. and Li, Q. (2019b), "Microstructures and mechanical properties of CrMnFeCoNi high entropy alloys fabricated using laser metal deposition technique", *Journal of Alloys and Compounds*, Vol. 773, pp. 387-392.

Xin, S., Shen, X., Du, C.C., Zhao, J., Sun, B.R., Xue, H.X., Yang, T.T., Cai, X.C. and Shen, T.D. (2021), "Bulk nanocrystalline boron-doped VNbMoTaW high entropy alloys with ultrahigh strength, hardness, and resistivity", *Journal of Alloys and Compounds*, Vol. 853, p. 155995.

Xu, X., Zhang, X., Chen, G. and Lu, Z. (2011), "Improvement of high-temperature oxidation resistance and strength in alumina-forming austenitic stainless steels", *Materials Letters*, Vol. 65 Nos 21/22, pp. 3285-3288.

Xu, Q.L., Zhang, Y., Liu, S.H., Li, C.J. and Li, C.X. (2020a), "High-temperature oxidation behavior of CuAlNiCrFe high-entropy alloy bond coats deposited using high-speed laser cladding process", *Surface and Coatings Technology*, Vol. 398, p. 126093.

Xu, Y., Li, Z., Liu, J., Chen, Y., Zhang, F., Wu, L., Hao, J. and Liu, L. (2020b), "Microstructure evolution and properties of laser cladding CoCrFeNiTiAlx high-entropy alloy coatings. ", *Coatings*, Vol. 10 No. 4, p. 373.

Yeh, J.W., Chen, S.K., Lin, S.J., Gan, J.Y., Chin, T.S., Shun, T.T., Tsau, C.H. and Chang, S.Y. (2004), "Nanostructured high-entropy alloys with multiple principal elements: novel alloy design concepts and outcomes", *Advanced Engineering Materials*, Vol. 6 No. 5, pp. 299-303.

Zelenitsas, K. and Tsakiropoulos, P. (2006), "Effect of Al, Cr and ta additions on the oxidation behaviour of Nb–Ti–Si in situ composites at 800 C", *Materials Science and Engineering: A*, Vol. 416 Nos 1/2, pp. 269-280.

Zhang, Y., Zuo, T., Cheng, Y. and Liaw, P.K. (2013), "High-entropy alloys with high saturation magnetization, electrical resistivity and malleability", *Scientific Reports*, Vol. 3 No. 1, pp. 1-7.

Zhou, Y., Zhang, Y., Wang, Y.L. and Chen, G.L. (2007), "Solid solution alloys of AlCoCrFeNiTix with excellent room-temperature mechanical properties", *Applied Physics Letters*, Vol. 90 No. 18, p. 181904.

Zhu, G., Liu, Y. and Ye, J. (2013), "Fabrication and properties of Ti (C, N)-based cermets with multi-component AlCoCrFeNi high-entropy alloys binder", *Materials Letters*, Vol. 113, pp. 80-82.

Zhu, J.M., Meng, J.L. and Liang, J.L. (2016), "Microstructure and mechanical properties of multi-principal component AlCoCrFeNiCu x alloy", *Rare Metals*, Vol. 35 No. 5, pp. 385-389.

About the authors

Modupeola Dada is a research student at the Tshwane University of Technology. Modupeola Dada is the corresponding author and can be contacted at: dadadupeola@gmail.com

Popoola Patricia is a Professor of metallurgy at the Tshwane University of Technology and the Leader of the Advanced Surface Engineering Research Centre at the same university in South Africa.

Ntombi Mathe is a doctor of philosophy in chemistry and the Senior Researcher at the Council of Scientific and Industrial Research, National Laser Center.

Sisa Pityana is a Professor of physics at the National Laser Centre, Council of Scientific and Industrial Research (NLC-CSIR) Centre, South Africa.

Samson Adeosun is a Professor in metallurgical and materials engineering at the University of Lagos, Akoka, Nigeria.